PERGAMON

Engineering Fracture Mechanics 66 (2000) 287–303

Engineering Fracture Mechanics

www.elsevier.com/locate/engfracmech

Compressional fractures considered as contact problems and mixed complementarity problems

J.-Cl. De Bremaecker[a,*], M.C. Ferris[b], D. Ralph[c]

[a]*Department of Geology and Geophysics, Rice University, Box 1892, Houston, TX 77251, USA*
[b]*Department of Computer Sciences, University of Wisconsin, Madison, WI 53706, USA*
[c]*Department of Mathematics, University of Melbourne, Parkville, Vic. 3052, Australia*

Received 8 April 1999; received in revised form 29 January 2000; accepted 6 February 2000

Abstract

The boundary conditions on the faces of compressional fractures are not known a priori since these faces may or may not be in contact, but the product of the normal stress and the normal relative displacement is necessarily null; similar but more complex conditions may be written for the shear stress and displacement. These conditions can be expressed in the form of a mixed linear complementarity problem. We use the Displacement Discontinuity Method and the PATH algorithm to solve them. This scheme is faster and more accurate than the methods previously used. The shear stresses on two parallel cracks depend on their separation, their inclination with respect to the imposed maximum compressional stress, and their geometry. The shear stress on two horizontal cracks separated by a small upward or downward step — considering the imposed direction of motion — drops to zero very near the step; in the case of a downward step this region is surrounded by a small region where the stress increases by a factor of about 10. Many more cases must be investigated before general conclusions can be drawn.

Keywords: Compressional fractures; Contact problems; Mixed complementarity problems

1. Introduction

Fracture mechanics has been mostly concerned with fractures whose faces are not in contact. For simplicity we will refer to such fractures as "open". While such fractures present many difficult problems, the boundary conditions (BC) on their faces are evident. For this reason, fracture mechanics has largely developed as a more or less independent discipline.

* Corresponding author. Tel.: +1-713-348-4886; fax: +1-713-285-5214.
E-mail address: deb@geophysics.rice.edu (J.Cl. De Bremaecker).

0013-7944/00/$ - see front matter
PII: S0013-7944(00)00022-9

There are, however, many cases in which it is not a priori known whether a fracture, or any part thereof, is open or closed: such is the case, for instance, in compressional fractures with "kinks", as well as in fractures at shallow depth in the Earth, where the pressure of the overlying rocks may keep some or all points of a fracture in contact. For simplicity we will refer to these problems as fracture contact problems. In these cases it is clear that the conditions on the crack faces are not ordinary boundary conditions; on the other hand, similar BC are encountered in contact problems with friction. (We will use the terms "fracture" and "crack" interchangeably.) Such problems are of great practical interest in engineering and industry, but the peculiar nature of their BC have made them very difficult to solve, see, e.g., [1–8].

This paper formulates the BC as a mixed complementarity problem. Such problems consist of pairs of inequalities, both of which must be satisfied, but with the caveat that at least one must hold as an equality (i.e., one of the inequalities is tight). Until recently, ad-hoc methods were used to solve these problems, essentially guessing which of the two inequalities should be tight, solving a system of equations, and a posteriori checking the other inequalities, modifying the guess, and repeating. The availability of the PATH algorithm [9–11] to solve mixed complementarity problems within a modeling system such as GAMS [12] has greatly improved this situation as the examples given here will demonstrate.

The benefits are three-fold. Firstly, the PATH algorithm (or other state-of-the-art complementarity solvers) is known to possess strong theoretical convergence properties (similar to those of damped Newton methods for nonlinear equations). The implementation uses sophisticated large-scale linear algebra techniques and has been well-tested on many different problems from a variety of disciplines [13]. Furthermore, since several different solvers are already linked to the modeling system, each of these solvers can be used interchangeably, by modifying a single statement in the model, rather than creating a new program for each new solver. Secondly, a modeling system enables a user to formulate the algebraic model in a manner that closely resembles the mathematical formulation given below (as compared to a Fortran implementation that typically obscures the physics). Thirdly, modeling systems provide a separation of model (equations) and data. Thus, each of the examples given in this paper use that same model with different data instantiations.

For further references on algorithms for frictional contact problems, see, e.g., [2]; some other references regarding the use of complementarity in engineering are given in [10,14,15].

The close connection between contact problems and complementarity problems, on the one hand, and fracture contact problems, on the other hand, appears to have first been noted by [16]; rather interestingly, this connection appears not to have been noted in the geological or geophysical literature.

2. Theory

Let us consider a finite elastic body, B, in static equilibrium under the action of known surface forces and/or displacements, i.e., boundary conditions. Body forces may also be present without affecting what follows.

The body contains several cracks; any point on these may be open or closed. It may be well to point out that these cracks are assumed to exist in the specified geometry in the body at rest; the application of the boundary conditions slightly alters their geometry, but does not cause them to propagate. Furthermore, these cracks may have any geometry, specifically, they need not be rectilinear, and may be at any distance from each other. In special cases it may be possible to determine which of these cracks or parts thereof are open or closed, but this is not generally true. For definiteness we will assume that the friction on the cracks is governed by a Coulomb-type relation, specifically, $|\tau| \leq -\mu \times \sigma$, where τ is the shear traction (or shear stress), μ is the friction coefficient, and σ is the normal traction (or normal

stress). Other friction laws could easily be accommodated. We will further assume that the usual elasticity conditions apply, i.e., that the stresses and strains are infinitesimal. We wish to determine the stresses and/or displacements on the cracks. Clearly, once this is done, these quantities can be determined anywhere in the body.

To solve the problem we first consider the case of two points P and P′ on opposite sides of the crack faces. When P and P′ are not in contact the tractions on the crack faces at P and P′ are obviously null. However, if P and P′ are in contact, the conditions are entirely different, since neither the tractions nor the relative displacements of P and P′ are known; let the normal component of the relative displacement of P and P′ be d_n, and its tangential component be d_s. Obviously, in this situation, $d_n = 0$, whereas $d_n < 0$ if P and P′ are not in contact. (We follow the sign convention introduced by Crouch and Starfield [17, p. 80] in which the separation of the faces is counted as negative; this convention is generally used in the Displacement Discontinuity Method.) Consequently, whether or not P and P′ are in contact, we have:

1. $\sigma \times d_n = 0$, since $\sigma = 0$ if the faces are not in contact, while $d_n = 0$ if they are; moreover,
2. $\sigma \leq 0$, counting compression as negative,
3. $d_n \leq 0$ (Signorini's condition).

These conditions are those of a linear complementarity problem [18], which here is a contact problem without friction. The presence of friction complicates the problem, in part because the friction law is governed by an inequality; correspondingly, we now deal with a mixed complementarity problem. The additional conditions resulting from friction are:

4. $|\tau| \leq -\mu \times \sigma$ (or some other definite relation),
5. if $|\tau| < -\mu \times \sigma$ then $d_s = 0$,
6. $\tau \times d_s \leq 0$ because, on the crack, the shear stress opposes the relative tangential velocity which has the same sign as the relative tangential displacement d_s.

These six conditions uniquely determine the solution. We can write them in the form of a linear mixed complementarity problem [9]. In what follows, we use the notation $\perp$ to signify that, in addition to the stated inequalities, one or other of the enclosing relationships is satisfied as an equality. For example, either $d_n = 0$ or $\sigma = 0$, and both of these are nonpositive. Note that all the stated relationships hold at an elemental level. These relationships are:

$$\begin{bmatrix} \tau \\ \sigma \end{bmatrix} = \mathbf{C}\,\mathbf{d}$$

where $\mathbf{C}$ is the matrix of influence coefficients [17, p. 94], and $d = [d_s, d_n]^T$.

$$d_n \leq 0 \perp \sigma \leq 0$$

$$d_s = d^+ - d^-$$

where d^+ and d^- are, respectively, the positive and negative parts of d_s. Finally,

$$-\mu \times \sigma \geq -\tau \perp d^+ \geq 0$$

$$-\mu \times \sigma \geq \tau \perp d^- \geq 0$$

These relationships guarantee the previously mentioned six conditions. Conditions 1, 2, and 3 correspond to the first two relationships above. For the friction cone constraints, we follow Lemma 1 of [19]. The two inequalities above involving σ and τ guarantee condition 4. Condition 5 follows from the

fact that if the two inequalities in σ and τ are both slack, then d^+ and d^- must be zero, and hence so is d_s. Finally, if $\tau > 0$, it follows that the first inequality involving σ and τ is slack, forcing $d^+ = 0$ by the complementarity relationship, hence $d_s \leq 0$, resulting in $\tau \times d_s \leq 0$. However, if $\tau < 0$, then the last relationship above implies $d^- = 0$, so that $d_s \geq 0$, giving again $\tau \times d_s \leq 0$.

As already noted, earth scientists developed solutions to fracture contact problems ($d_n = 0$) essentially independently from the work done in other sciences; their methods are now briefly summarized:

- Obviously the simplest solution to the problem is obtained by assuming that the friction on the crack(s) vanishes [20]; the applicability of the results thus obtained can not be easily determined in most cases.
- The value of σ, τ, d_n or d_s have sometimes been prescribed [21–23] although the error of doing so appears to have been suspected [24].
- The method most often used is given by Crouch and Starfield [17, pp. 205–276]. It consists, essentially, in introducing supplementary elements ("joint elements") in the crack where the crack faces are in contact. The thickness (h) of these elements is small, but cannot be zero, and their normal and shear stiffnesses (K_n and K_s) are high compared to those of the body. Special provision must be made to simulate the friction law. In general, though, it is not known which elements on the crack faces are in contact because of the interaction between τ (and d_s) and σ (and d_n); how the choice of h, K_n and K_s affect the accuracy of the solution is similarly unknown. Finally, the iterations necessary to simulate the friction law have been found to converge for simple crack geometry, but proof of convergence in the general case is lacking. Nevertheless, because of its simplicity, this method has been rather widely used, e.g., [25–28].
- Finally, attempts have been made to arrive at the correct BC by more or less systematically decreasing the separation between the crack faces [3,6,7,29]. Absent a realization of the complementary nature of the BC, these attempts were only mildly successful.

3. Numerical method

Both the finite element method (FEM) and the boundary element method (BEM) and its variants may be used to solve the problem. The FEM is clearly preferable if the body is inhomogeneous and/or if two bodies are in contact. It will not be discussed here. The BEM as such cannot solve fracture problems due to the inherent impossibility of distinguishing forces applied on one side of the crack from these on the opposite side. A version of the BEM known as the Dual Boundary Element Method [30,31] has, however, been used.

An appreciably simpler version of the BEM, however, has long been available: the Displacement Discontinuity Method (DDM) [17,32, pp. 79–109]. The advantage of this method for the present problem is that the displacement discontinuities which it uses, are exactly those which were considered in the previous paragraph. On the other hand, in common with all BEM methods, it is ill-suited to the treatment of inhomogeneous bodies. Finally, a theoretical error analysis for the DDM is not available. It should also be mentioned that the ability to consider infinite bodies, which is an important advantage of all BEM methods, may appear not to exist when using the present method: specifically, the fractures must be embedded in a finite body. The reason will be obvious by considering the conditions which have to be fulfilled on the fractures: the simplest solution to these is $\sigma = \tau = d_n = d_s = 0$ at all points on the fractures. In the absence of the usual BC on the surface of the body, this is the solution to the problem. This apparent restriction is, however, of little real importance: with an appropriate choice of traction BC the size of the body does not affect the solution.

Using an updated version of the program TWODD [17, pp. 293–303], see [3], as our point of departure, we implemented the six conditions listed above in the GAMS language [12] and using the PATH algorithm. For a simple overview of the use of these tools for engineering and mechanics, the reader is referred to [33]. Here, we will just give a description of the basic features of the computational method used.

In its simplest instantiation, the complementarity problem takes two inequalities and forces one of them to be satisfied as an equation. In our example, $d_n \leq 0$ and $\sigma \leq 0$, and either $d_n = 0$ or $\sigma = 0$. Algorithms for complementarity satisfy the inequalities precisely, and determine in the solution process which of the inequalities to satisfy as an equation. There are many algorithms for solving these problems, see for example the surveys [34,35]. The PATH algorithm [9–11] is based on a homotopy approach, whereby a piecewise linear approximation of an equivalent non-smooth equation is solved in an iterative fashion. The convergence theory [36] is based on a generalization of Newton's method; some comparison to other solvers can be found in [13].

The solution of the problem takes very little time, e.g., about 2 min for a problem with 300 elements on a SparcUltra1/140, but the time taken varies with the "difficulty" of the problem. While some of the examples below use only few elements (of the order of 10 on each crack) and simple geometrical configurations, others use an irregular geometry with as many as 100 elements on each crack (280 total), and with the elements gradually decreasing in size. The latter problems are difficult to solve, and may result in very rapid variations of the tractions on the crack, as will be shown below; consequently they provide a good illustration of the efficiency of the present scheme.

One important remark must be made: since the solution of the problems considered cannot be obtained analytically, the only practical criterion to ensure that the solution obtained is "correct" is to increase the number of elements until the solution no longer changes appreciably. The same remark applies, of course, to most other numerical methods: it has nothing to do with the algorithm used to find the solution, instead it is simply due to the errors inherent in the numerical method itself. In some cases which we have investigated, the solution obtained when the number of elements was much smaller than the previous criterion requires, was extremely different from the correct one. The only other general rules appear to be that the elements on the surface of the body may be relatively long provided that:

1. The BC on these elements do not vary, and;
2. The length of each element is much smaller than its distance from the cracks.

Our code enables us gradually to vary the size of elements in any segment; this is advantageous in modeling small-scale phenomena (see Section 4.3 below).

4. Results

Because of the ease with which results are obtained and the variety of models which can be investigated, we will give only a few results for models which appear to be of some general interest. The code is still being developed to be able to present results more comprehensively and conveniently, and to treat different problems.

4.1. Two parallel right-stepping cracks under compression

In these first models we wish to determine the shear stresses on two parallel cracks inclined at various angles (β) to the horizontal and whose normal separation (sep.) varies. (The latter is the distance between the cracks along their normal.) These cracks are referred to as "right-stepping" in the

geological literature because an observer standing on either crack and looking towards its end must step, or look, to the right to get to the other crack. A typical case (File name: *two-15a*, $\beta = 15^\circ$, sep = 2.28) is shown in Fig. 1. (The cracks and the angle β are shown in the inset.) Each crack is 11.18 long. (All the parameters are shown in Table 1.) The cracks are embedded in a rectangular body, hereinafter referred to as a "box", 160 wide (E–W dimension) and 150 long. (The unit length is arbitrary.) The sides are subject to an inward normal displacement of 0.1 and no tangential displacement, the top and bottom are traction-free. All these parameters are kept constant, but the normal separation of the cracks is gradually increased from 2.28 to 3.35, 4.47, 6.71 and finally to 8.94. There are only five elements along the top, bottom and each side, and 12 along each crack; the effects of this small number of elements will be examined later.

4.1.1. $\beta = 15^\circ$ (Fig. 2)

The geometry of the cracks at the separations listed above is shown in the inset of Fig. 2; the figure

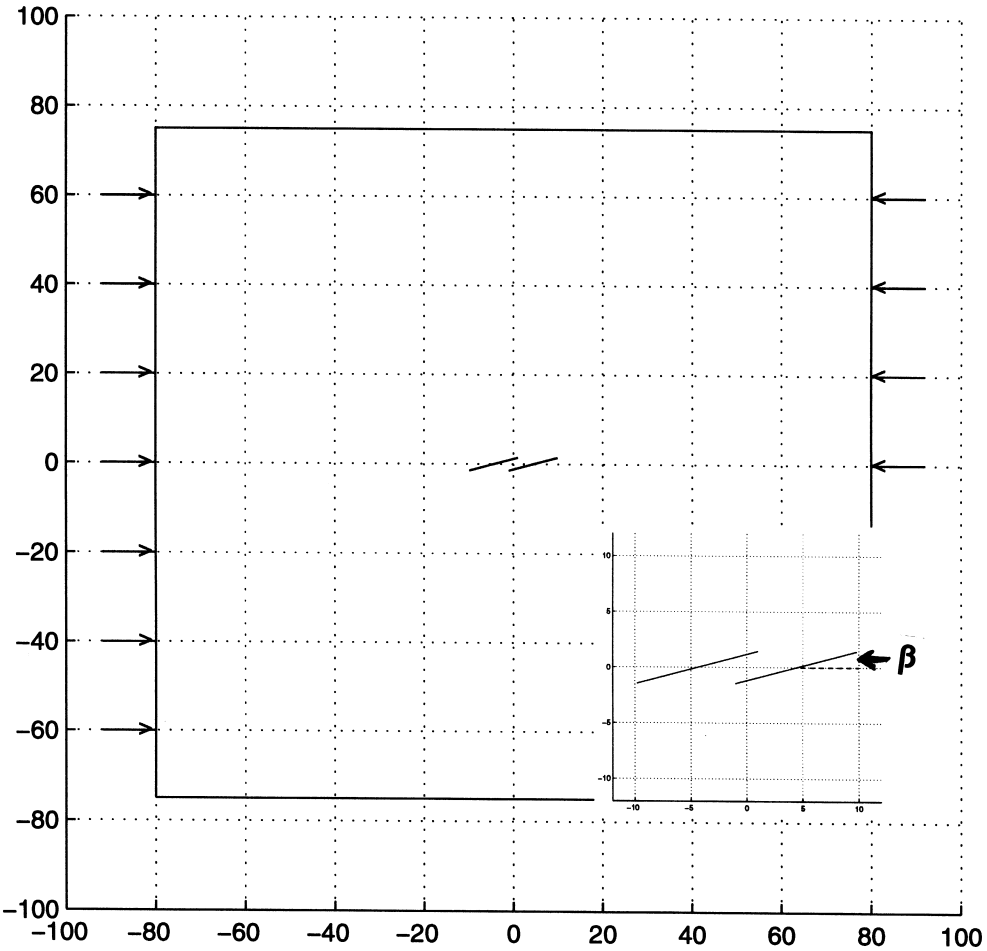

Fig. 1. The box, 160 × 150 and the two embedded right-stepping cracks, each 11.18 long, inclined at 15° and separated by 2.28, and a sketch of the boundary conditions (BC) (file name: *two-15a*, see Table 1). Inset: the two cracks and the angle β.

itself shows the value of the shear stress τ along the cracks vs. the horizontal coordinate x of the centers of the elements for these separations. At minimal separation (File name: *two-15a*, solid lines in the inset, symbol ○ in the main figure), τ completely vanishes near $-2 < x < 2$. This phenomenon is obviously due to the proximity of the two cracks, indeed the inset shows that both cracks co-exist in this range of x. The main figure shows that the proximity effect gradually decreases as the separation increases (File names: *two-15b* to *two-15e*), and amounts to about 10% for a separation of 8.94 (lines ending with a star in the inset, symbol $*$ in the main figure).

4.1.2. $\beta = 26.6^\circ$ (Fig. 3)

The geometry of the cracks at the various separations (File names: *two-26a* to *two-26e*) is shown in the inset of Fig. 3, and the value of τ along the cracks vs. x is shown in the main figure. The geometry immediately suggests that the proximity effect should be much more pronounced than for $\beta = 15^\circ$, and

Table 1
Data for the models[a]

Name	Fig.	E–W	n	N–S	p	μ	β	L	q	grad	Type	Remarks	BC
two-15a	1–2	160	5	150	5	0.5	15.0	11.18	12	1.0	R.S.	sep. = 2.28	*D*
two-15b	1–2	160	5	150	5	0.5	15.0	11.18	12	1.0	R.S.	sep. = 3.42	*D*
two-15c	1–2	160	5	150	5	0.5	15.0	11.18	12	1.0	R.S.	sep. = 4.56	*D*
two-15d	1–2	160	5	150	5	0.5	15.0	11.18	12	1.0	R.S.	sep. = 6.71	*D*
two-15e	1–2	160	5	150	5	0.5	15.0	11.18	12	1.0	R.S.	sep. = 8.94	*D*
two-26a	3	160	5	150	5	0.5	26.6	11.18	12	1.0	R.S.	sep. = 2.28	*D*
two-26b	3	160	5	150	5	0.5	26.6	11.18	12	1.0	R.S.	sep. = 3.42	*D*
two-26c	3	160	5	150	5	0.5	26.6	11.18	12	1.0	R.S.	sep. = 4.47	*D*
two-26d	3	160	5	150	5	0.5	26.6	11.18	12	1.0	R.S.	sep. = 6.71	*D*
two-26e	3	160	5	150	5	0.5	26.6	11.18	12	1.0	R.S.	sep. = 8.94	*D*
two-35a	4	160	5	150	5	0.5	35.0	11.18	12	1.0	R.S.	sep. = 2.28	*D*
two-35b	4	160	5	150	5	0.5	35.0	11.18	12	1.0	R.S.	sep. = 3.42	*D*
two-35c	4	160	5	150	5	0.5	35.0	11.18	12	1.0	R.S.	sep. = 4.56	*D*
two-35d	4	160	5	150	5	0.5	35.0	11.18	12	1.0	R.S.	sep. = 6.71	*D*
two-35e	4	160	5	150	5	0.5	35.0	11.18	12	1.0	R.S.	sep. = 8.94	*D*
two-35a-L	5a	160	5	150	5	0.5	35.0	11.18	12	1.0	L.S.	sep. = 2.28	*D*
two-35b-L	5a	160	5	150	5	0.5	35.0	11.18	12	1.0	L.S.	sep. = 3.42	*D*
two-35c-L	5a–b	160	5	150	5	0.5	35.0	11.18	12	1.0	L.S.	sep. = 4.56	*D*
two-35d-L	5b	160	5	150	5	0.5	35.0	11.18	12	1.0	L.S.	sep. = 6.71	*D*
two-35e-L	5b	160	5	150	5	0.5	35.0	11.18	12	1.0	L.S.	sep. = 8.94	*D*
one-35	5b	160	5	150	5	0.5	35.0	11.18	12	1.0		single crack	*D*
test7	7	90	20	20	20	0.5	0.0	10.0	40	0.85	up	0.01	*T*
test7b	7	90	20	40	20	0.5	0.0	10.0	40	0.85	up	0.01	*T*
test7c	7	90	20	40	20	0.5	0.0	10.0	100	0.85	up	0.01	*T*
test8	7	90	20	20	20	0.5	0.0	10.0	100	0.85	up	0.01	*T*
test9b	8	90	20	40	20	0.5	0.0	10.0	40	0.85	dw	0.01	*T*
test10b	8	90	20	40	20	0.5	0.0	10.0	100	0.85	dw	0.01	*T*

[a] Name: for identification only; Fig.: figure numbers; E–W: length in the horizontal or east–west direction; n: number of elements in this direction; N–S: length in the vertical or north–south direction; p: number of elements in this direction; μ: coefficient of friction; β: angle of the cracks with the horizontal direction; L: length of each crack; q: number of elements on each crack; grad: decrease of the element size towards the step for horizontal cracks; Type: R.S.: right stepping cracks, L.S.: left stepping cracks, up: the step is upward in the direction of motion, dw: the step is downward in the direction of motion; Remarks: sep.: separation along the normal to the cracks, single crack: self-explanatory, 0.01: size of the step between the cracks; BC: boundary conditions on the box, *D*: displacement BC on N–S sides, *T*: traction BC on all sides (see text for details). Young's modulus = 1.0 and Poisson's ratio = 0.25 in all models.

this is indeed the case, although the proximity effect is again small at maximum separation, i.e., 8.94 (*two-26e*, lines ending with a star in the inset, symbol $*$ in the main figure).

As previously mentioned, we have examined the effect of the number of elements and of the size of the box.

- If we increase the number of elements along both top, bottom and each side from 5 to 15 and along each crack from 12 to 40, the maximum difference in the shear stresses is only 5%.
- If we reduce the size of the box from 160×150 to 50×45 (while keeping 40 elements on each crack) and compare the results obtained with 15 and with five elements along top, bottom and each side, the results change by 12% at the most. Note that in the latter case each element is 9 or 10 long, and is thus, relatively close to the cracks, but this unfavorable configuration has only a minor influence on the results.

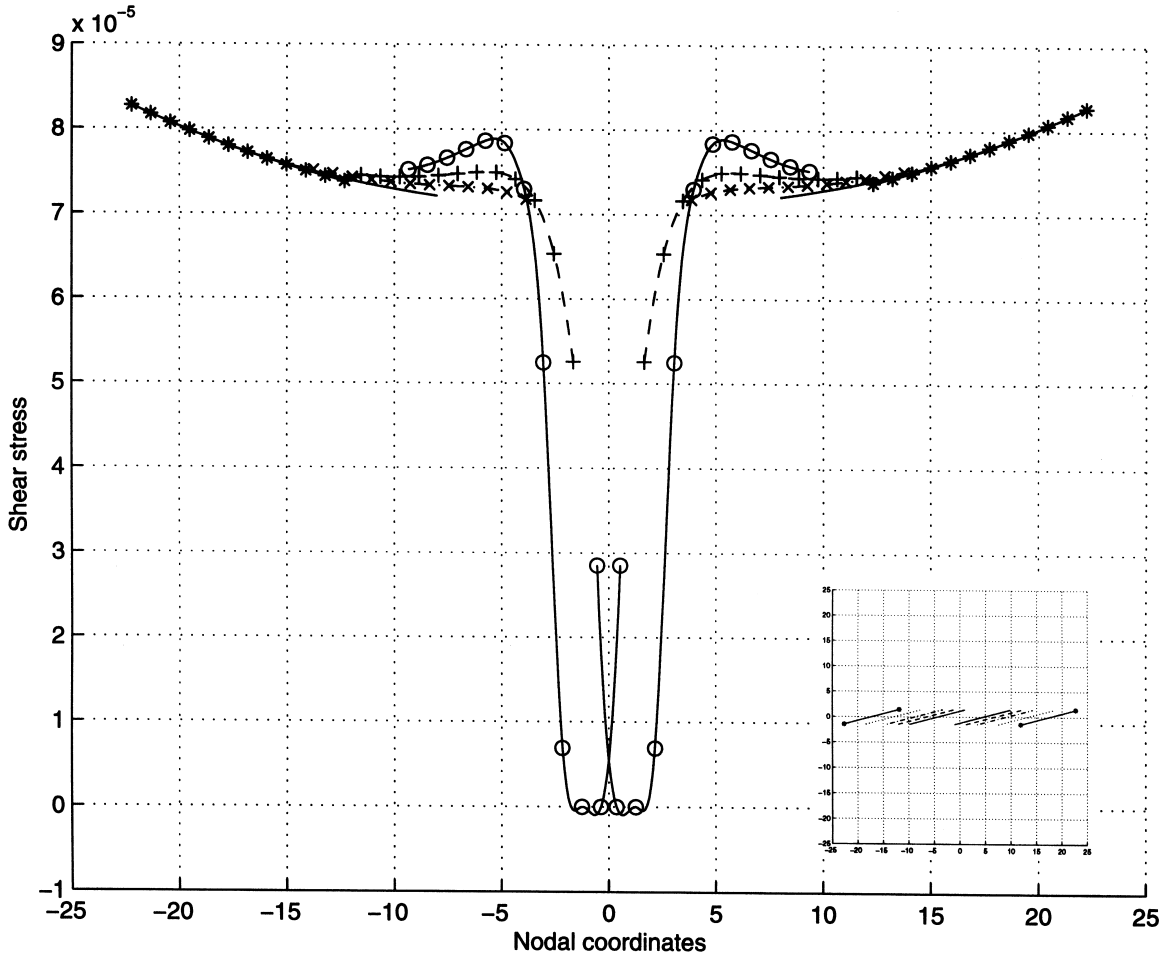

Fig. 2. Shear stresses on right-stepping cracks inclined at 15° as shown in the inset. Separation 2.28: symbol ○; 3.42 symbol +; 4.56 symbol ×; 6.71 symbol −; 8.94 symbol $*$. In the inset the lines are, respectively, solid, dashed, dash-dottted, dotted, and ending with a star (file names: *two-15a* to *two-15e)*.

4.1.3. $\beta = 35^\circ$ (Fig. 4)

Here the geometry of the cracks is shown in the inset of Fig. 4, and the value of τ in the main figure (Files: *two-35a* to *two-35e*). The same symbols are used as in Fig. 3. The point here is that the proximity effect is still very appreciable even at the largest separation, i.e., 8.94 (*two-35e*, lines ending with a star in the inset, symbol $*$ in the main figure). It should be added that this effect is not due to the small numbers of elements: computations with 15 elements on top, bottom and each side and 40 on each crack yield practically identical results.

4.2. Two parallel left-stepping cracks under compression (Fig. 5(a) and (b))

Since the previous examples clearly show that the stresses on parallel cracks cannot be simply predicted, and since such models could be varied at infinity, we will examine only one series of other cases in which $\beta = 35^\circ$, but with "left-stepping" instead of "right-stepping" cracks (*two-35a-L* to *two-35e-L*). All the other parameters are the same as for the right stepping cracks. The geometry of the

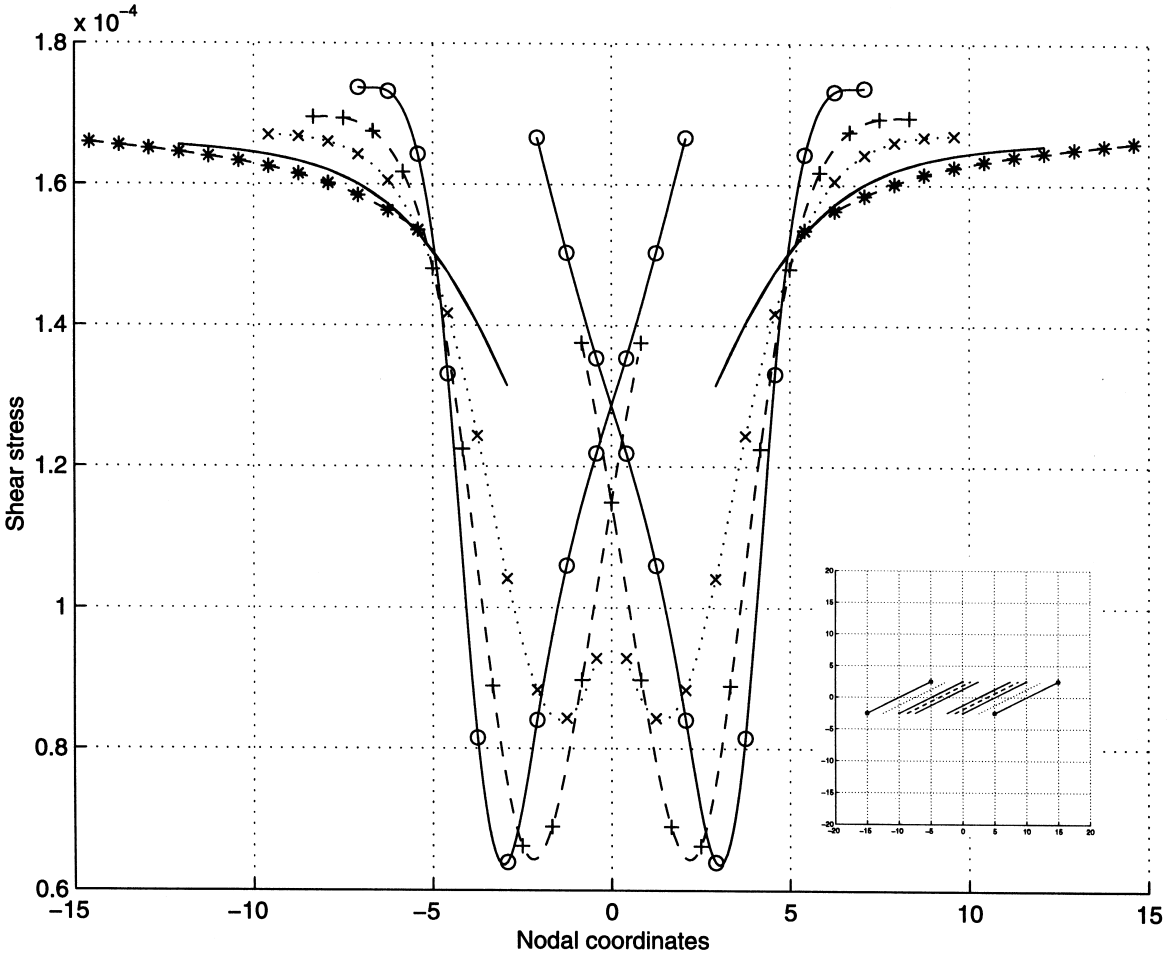

Fig. 3. Shear stresses on right-stepping cracks inclined at 26.6°as shown in the inset. Symbols as in Fig. 2 (*two-26a* to *two-26e*).

cracks is shown in the insets of Fig. 5(a) and (b), and the variation of τ along the cracks in the main figures; two figures were necessary because of the unexpectedly complex pattern. As can be seen, the proximity effect is quite large even at the greatest separation (symbol $*$ in Fig. 5(b)). For reference purposes the shear stress ($\tau \approx 2.5 \times 10^{-4}$) on a single crack is shown by the heavy line on Fig. 5(b). Remarkably, at minimal separation (*two-35a-L*, symbol ○ in Fig. 5a) the curve of τ vs. x presents an almost flat part near $x = 0$ at this same value. It is not easy to understand the reason therefor, since it does not occur for right-stepping cracks.

4.3. Effect of a small step, or asperity, along a crack

In real materials, fractures are far from being smooth, but the effect of such roughness is difficult to estimate. The term asperity has been used with different meaning in different fields [37, p. 217]. As a first step toward such an investigation we computed the effect of a small step, either "up" or "down" between a pair of horizontal cracks. Alternatively, these cracks can also be considered left- and right-

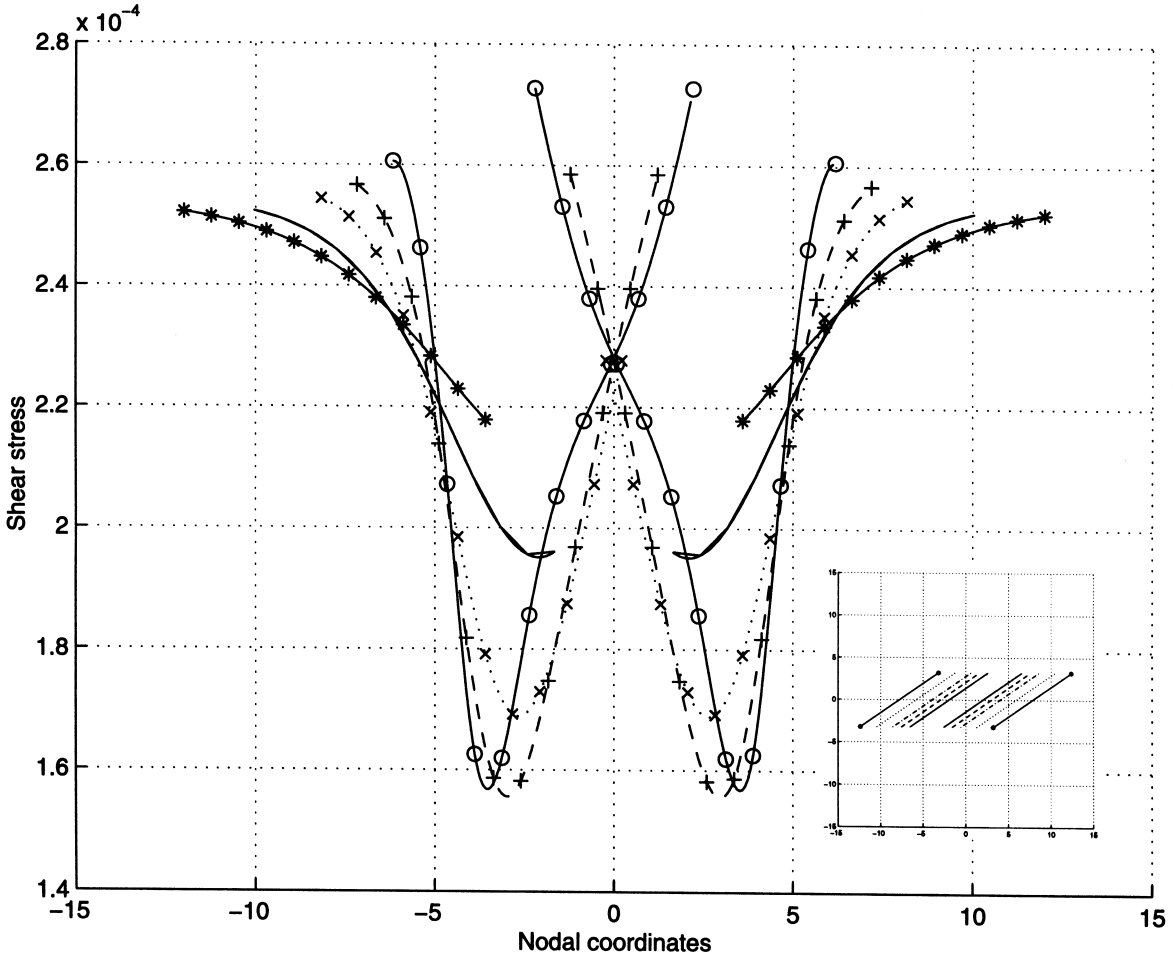

Fig. 4. Shear stresses on right-stepping cracks inclined at 35° as shown in the inset. Symbols as in Fig. 2 (*two-35a* to *two-35e*).

stepping, respectively. Each crack is 10.0 long and the step is 0.01; both cracks extend from ± 10.0 to 0.0. At the top and bottom of the box (20 elements each) we impose $\sigma = -5.0 \times 10^{-4}$, and $\tau = 6.6 \times 10^{-4}$ (τ tends to make the top move to the right and the bottom to the left). On both sides (also 20 elements each), we impose $\tau = -6.6 \times 10^{-4}$. In order to prevent translation and rotation, a small segment inside the box is constrained not to move.

4.3.1. An upward step

We will first examine the case in which the box is 90×40 (*test7b* and *test7c*). The box and the cracks are shown in the inset of Fig. 6 (solid lines), the cracks themselves in the main figure; in the latter the step has been magnified by a factor of 100 to make it visible. Since the upward step between the two

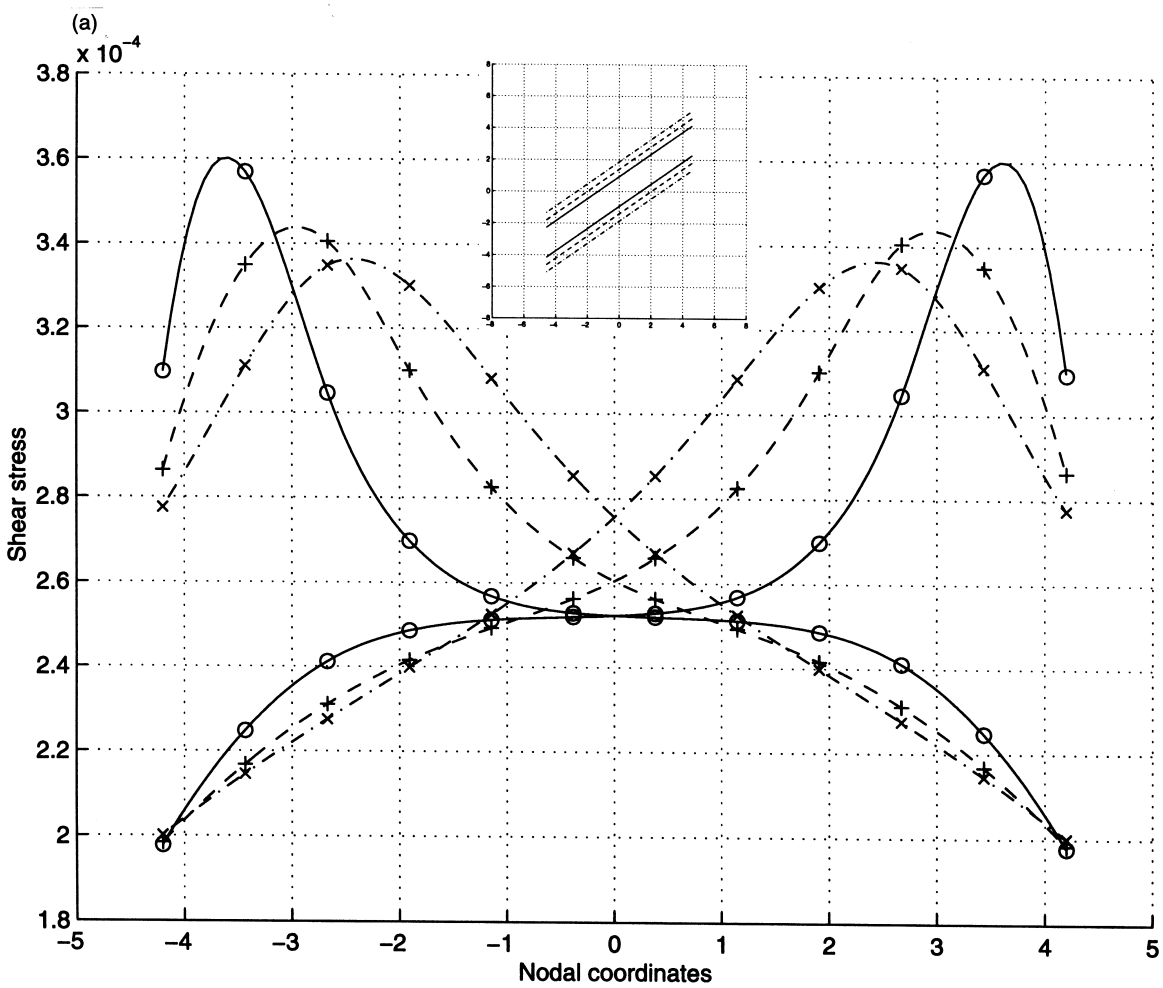

Fig. 5. (a) Shear stresses on three left-stepping cracks inclined at 35° with the three least separations as shown in the inset. Symbols as in Fig. 2 *(two-35a-L* to *two-35c-L)*. (b) Shear stresses on three left-stepping cracks inclined at 35° with the three greatest separations shown in the inset. Symbols as in Fig. 2 *(two-35c-L* to *two-35e-L)*. The heavy horizontal line is the shear stress on a single crack *(one-35)*.

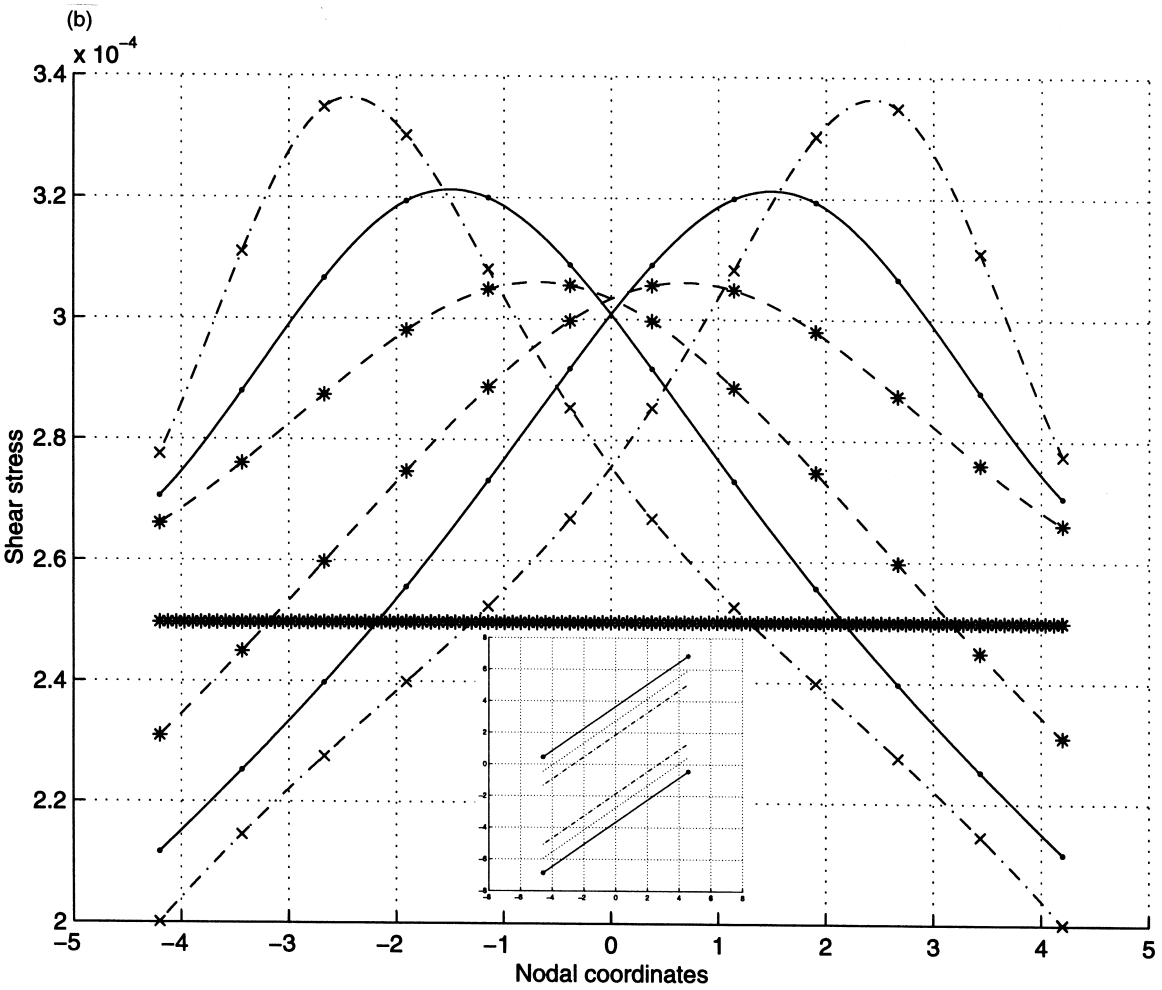

Fig. 5 (*continued*)

cracks is only 0.001 of each crack length, extremely small elements must be used in its vicinity. This is accomplished by automatically decreasing the size of the elements towards the step by a factor of 0.85. With 40 elements (*test7b*) on each crack the element nearest to the step is less than 3×10^{-3} long, with 100 elements (*test7c*) this length decreases to 3.3×10^{-7}.

One might be tempted simply to say that this case corresponds to a step "up" (left-stepping); what is important, however, is the following: looking in the direction of motion imposed on the top of the box (i.e., to the right in Figs. 6 and 7) one sees that the second crack is displaced upward with respect to the first one. The result, shown in Fig. 7 (symbol $+$), may be unexpected. (Only the central part of the cracks is shown because τ remains essentially constant and approximately 2.5×10^{-4} for $|x| > 1$): τ drops to zero at a distance of about 0.2 from the step (*test7b*, symbol $*$); correspondingly, the crack faces are not in contact in this region.

The unforeseen character of this result led us to suspect that it was due to an insufficient number of

elements on the cracks, but such is not the case: when the result is recomputed with 100 elements on the cracks (rather than 40) (*test7c*, symbol +) there is no appreciable change.

On the other hand, if one reduces the size of the box to 90 by 20, as shown by the dashed lines in the inset of Fig. 6, (*test7* and *test8*) the region in which τ drops to zero is somewhat increased: the symbols ○ and × on Fig. 7 correspond, respectively, to 40–100 elements on the crack. It is intuitively clear that the box shown by the dashed lines of the inset of Fig. 6 is not likely to lead to very accurate results, but the smallness of the differences due to the two box sizes is encouraging.

4.3.2. A downward step

If all the parameters of the previous case are left unchanged except that the second crack is displaced downward with respect to the first (considering the motion imposed on the top of the box), (see inset of Fig. 8, where the step has been magnified by a factor of 100 to make it visible) the pattern is even more remarkable (*test9b* and *test10b*; Fig. 8, symbols ○ and ×): τ first increases by a factor of about 11 at a distance of about 0.14 from the step, and then drops to zero at a distance of 0.007 from it. Here also an

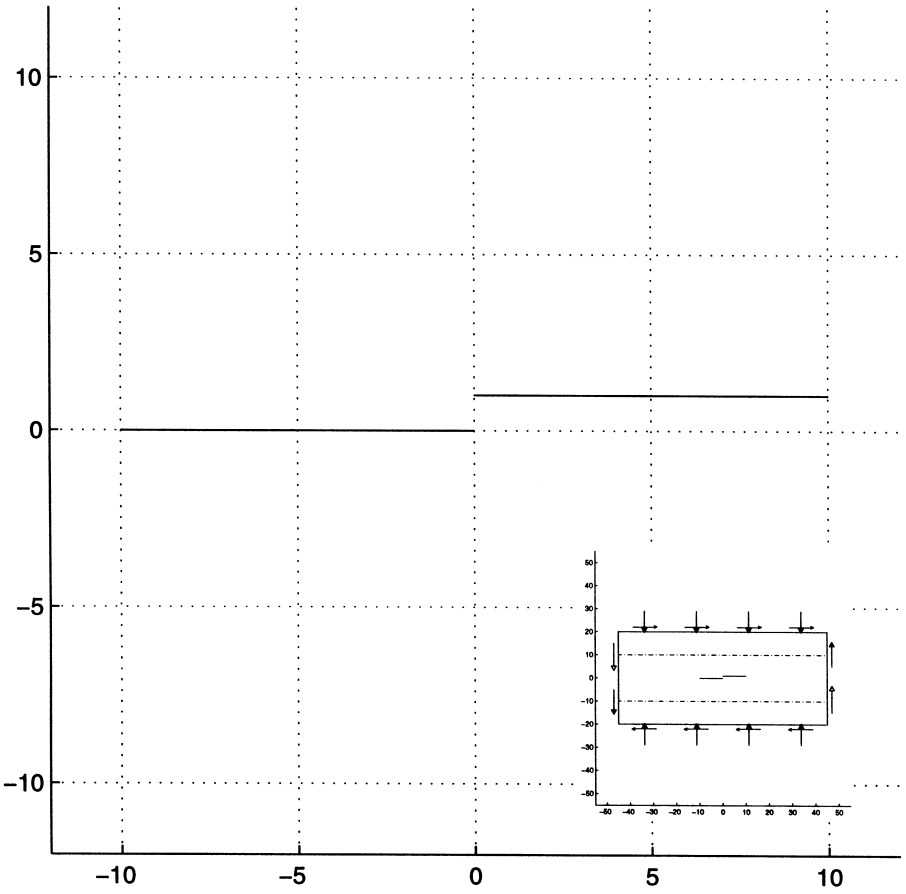

Fig. 6. Two horizontal cracks, each 10 long, separated by an upward step of 0.01; the step has been magnified by a factor of 100 for clarity. Inset: the box, 90 × 40 (solid lines) and 90 × 20 (dashed horizontal lines and solid vertical lines), the two horizontal cracks, and a sketch of the BC (see text and Table 1 for details).

increase in the number of crack elements from 40 (symbol ○) to 100 (symbol ×) has no measurable influence on the results; it seems thus highly probable that they are correct. This conclusion is strengthened by the fact that these results were obtained by starting with only 10 elements on each crack, then increasing this number to 20, and then 40 until it became clear that the number of elements no longer affected the results.

It should be added that if the "step" of size 0.01 is replaced by a "gap" of the same size, i.e., if the two cracks are in perfect alignment, τ remains constant at 2.5×10^{-4} within 1 part in 2.8×10^{4}, thus strengthening the conclusion that the results shown in Figs. 7 and 8 are correct. It is hoped that further research on this subject will contribute to clarifying the role of asperities, especially in geophysics.

We believe that the effect of asperities would not be easily modeled by other methods, and thus provide excellent examples of the efficiency of the PATH algorithm and of the mixed complementarity approach.

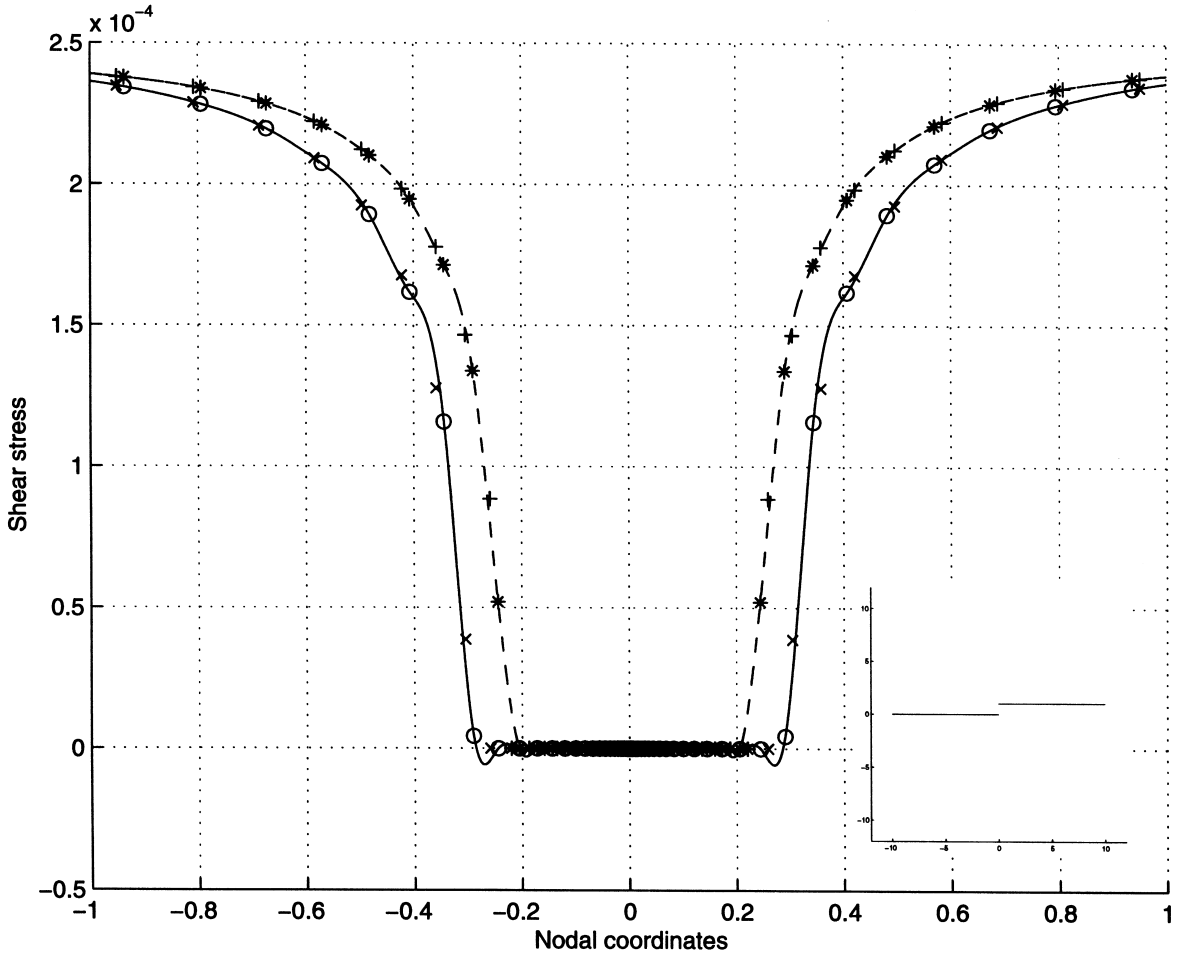

Fig. 7. Shear stresses on central parts of the cracks shown in Fig. 6. The symbols ∗ and + show, respectively, the results with 40 and 100 crack elements for a box 90×40 (*test7b* and *test7c*); the symbols ○ and × do the same but for a box 90×20 (*test7* and *test8*). Inset: The two cracks and the step magnified by 100.

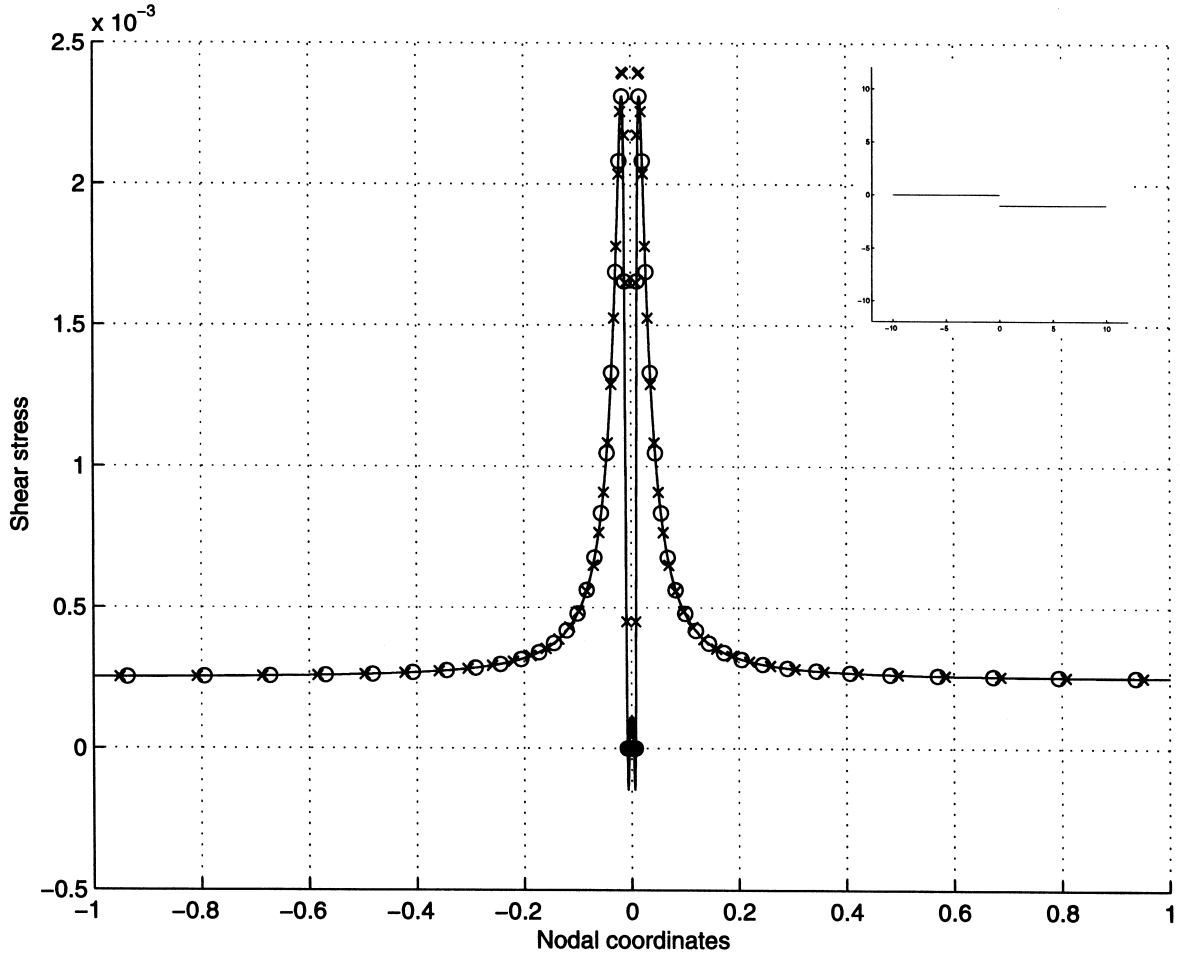

Fig. 8. Shear stresses on cracks similar to those shown in Fig. 7 but with a downward step. The symbols ○ and × show, respectively, the results with 40 (*test9b*) and 100 elements (*test10b*) on the cracks. The box is 90 × 40. Inset: The two cracks and the step magnified by 100.

5. Conclusions

The stresses on parallel compressional cracks can now easily be computed using the PATH algorithm and the Displacement Discontinuity Method, although other numerical methods could also be used. The results depend both on the spacing of the cracks, their inclination with respect to the direction of maximum compressive stress, and their geometry.

This same method was used to investigate the effect of a small step up or down on a crack. We find that the shear stress drops to zero very near the step. Moreover, if the step is downward — considering the direction of motion — this drop may be surrounded by a small region in which the stress increases by a factor of approximately 10. Such cases provide good examples of the efficiency of the present scheme.

Many more cases must be investigated before general conclusions can be drawn.

Note added in proof

The paper by Elvin and Leung [38] which treats the same problem was, unfortunately, published too late to be mentioned in the main body of the present paper.

Acknowledgements

This work was supported by NSF Grant No. CCR-9619765 to M.C.F. Computer time was made available by the Department of Geology and Geophysics, Rice University. We wish to thank John Dennis of Rice University for putting us in touch with one another. The comments of two anonymous referees substantially improved the manuscript.

References

[1] Chabrand P, Dubois F, Raous M. Various numerical methods for solving unilateral contact problems with friction. Mathematical and Computer Modelling 1998;28:97–108.
[2] Christensen PW, Klarbring A, Pang JS, Strömberg N. Fomulation and comparison of algorithms for frictional contact problems. Int J Numer Meth Engrg 1998;42:145–73.
[3] De Bremaecker J-Cl. Numerical models of shear crack propagation using the displacement discontinuity method. In: Aliabadi MH, editor. Fracture of rock. Boston: WIT Press, 1999. p. 23–38.
[4] Mistakidis ES, Panagouli OK, Panagiotopoulos PD. Unilateral contact problems with fractal geometry and fractal friction law; methods of calculation. Computational Mechanics 1998;21:353–62.
[5] Refaat MH, Meguid SA. A new strategy for the solution of frictional contact problems. Int J Numer Meth Engrg 1998;43:1053–68.
[6] Wei K, De Bremaecker J-Cl. Fracture growth. Part II: Case studies. Geophys J Int 1995;122:746–54.
[7] Wei K, De Bremaecker J-Cl. Fracture growth. Part I: Formulation and implementations. Geophys J Int 1995;122:735–45.
[8] Zavarise G, Wriggers P, Schrefler BA. A method for solving contact problems. Int J Numer Meth Engrg 1998;42:473–98.
[9] Dirkse SP, Ferris MC. The PATH solver: a non-monotone stabilization scheme for mixed complementarity problems. Optimization Methods and Software 1995;5:123–56.
[10] Ferris MC, Pang JS. Engineering and economic applications of complementarity problems. SIAM Review 1997;39:669–713.
[11] Ferris MC, Munson TS. Complementarity problems in GAMS and the PATH solver. J. of Economics Dynamics and Control 1999;24:165–88.
[12] Brooke A, et al. GAMS, A user's guide. Washington, DC: GAMS Development Corp, 1998. 262 pp.
[13] Billups SC, Dirkse SP, Ferris MC. A comparison of large scale mixed complementarity problem solvers. Computational Optimization and Applications 1997;7:3–25.
[14] Dirkse SP, Ferris MC. MCPLIB: a collection of nonlinear mixed complementarity problems. Optimization Methods and Software 1995;5:319–45.
[15] Ferris MC, Pang JS, editors. Complementarity and variational problems: State of the art. Philadelphia, PA: SIAM Publications, 1997 473 pp.
[16] Gringauz M. On mathematical-programming formulation for contact crack problems. Int J Fract 1993;60:R3–R7.
[17] Crouch SL, Starfield AM. Boundary element methods in solid mechanics. London: George Allen and Unwin, 1983 (reprinted, 1990) 322 pp.
[18] Cottle RW, Pang J-S, Stone RE. The linear complementarity problem. London: Academic Press, 1992 762 pp.
[19] Pang JS, Trinkle JC. Complementarity formulations and existence of solutions of multi-rigid-body contact problems with Coulomb friction. Mahematical Programming 1996;73:199–226.
[20] Willemse JM, Pollard DD, Aydin A. Three-dimensional analyses of slip distributions on normal fault arrays with consequences for fault scaling. J Struct Geol 1996;18:295–309.
[21] Pollard DD, Segall P. Theoretical displacements and stresses near fractures in rock: with application to faults, joints, veins, dikes, and solution surfaces. In: Atkinson BK, editor. Fracture mechanics of rock. San Diego, CA: Academic Press, 1987. p. 277–349.
[22] Segall P, Pollard DD. Mechanics of discontinuous faults. J Geophys Res 1980;85:4337–50.

[23] Crider JG, Pollard DD. Fault linkage: three-dimensional mechanical interaction between échelon normal faults. J Geophys Res 1998;103:24,373–91.
[24] Zeller SS, Pollard DD. Boundary conditions for rock fracture analysis using the boundary element method. J Geophys Res 1992;97:1991–7.
[25] Cooke ML. Fracture localization along faults with spaially varying friction. J Geophys Res 1997;22,425–34.
[26] Cooke ML, Pollard DD. Bedding-plane slip in initial stages of fault-related folding. J Struct Geol 1997;19:567–81.
[27] Aydin A, Schultz RA. Effect of mechanical interaction on the development of strike-slip faults with echelon pattern. J Struct Geol 1990;12:123–9.
[28] Schultz RA, Aydin A. Formation of interior basins associated with curved faults in Alaska. Tectonics 1990;9:1387–407.
[29] De Bremaecker JCl, Wei K. The propagation of a single shear crack: a displacement discontinuity model. Pure Appl Geophysics (Special issue on Rock Friction, Faulting and Earthquake Mechanics) 1994;142:567–85.
[30] Portela A. Dual boundary element analysis of crack growth. In: Brebbia CA, Connor JJ, editors. Topics in Engineering, vol. 14. Boston: Computational Mechanics Publications, 1993 176 pp.
[31] Wilde AJ, Aliabadi MH. Boundary element analysis for rock fracture. In: Aliabadi MH, editor. Fracture of Rock. Boston: WIT Press, 1999. p. 1–21.
[32] Crouch SL. Solution of plane elasticity problems by the displacement discontinuity method. Int J Numer Meth Engrg 1976;10:301–43.
[33] Tin-Loi F, Ferris MC. Complementarity problems in engineering and mechanics: Models and solution. Madison, WI: Computer Sciences Department, University of Wisconsin, 1998.
[34] Harker PT, Pang JS. Finite-dimensional variational inequality and nonlinear complementarity problems: a survey of theory, algorithms and applications. Mathematical Programming 1990;48:161–220.
[35] Ferris MC, Kanzow C. Complementarity and related problems: A survey. Madison, WI: Computer Sciences Department, University of Wisconsin, 1998.
[36] Ralph D. Global convergence of damped Newton's method for nonsmooth equations via the Path search. Mathematics of Operations Research 1994;19:352–89.
[37] Scholz CH. The mechanics of earthquakes and faulting. Cambridge: Cambridge University Press, 1990 439 pp.
[38] Elvin N, Leung C. A fast iterative boundary element method for solving closed crack problems. Engineering Fracture Mechanics 1999;63:631–48.